Experimental and theoretical investigations of a hybrid solar heating system with ground storage

Contents

Abstract

A hybrid solar heating system with ground storage is investigated experimentally in a laboratory test facility by means of detailed measurements during one year of operation. The experimental investigations are performed with weather of 2018 – 2019 and space heating and domestic hot water consumption corresponding to a low energy single-family house. In addition, a numerical model of the system is built in TRNSYS. The model is validated against the measurements.

The results show a very high degree of similarity between the measurements and the calculations with the validated TRNSYS model and yearly performances of the investigated system and the optimized system are calculated with the model.

Keywords Solar heating/heat pump system, Ground storage, Experimental investigations, Model validation and Seasonal performance factor.

Introduction and background

Energy systems outside the district heating network area must in the future be operated with 100 % renewable energy and be able to cover the total heating demand in buildings in the most energy saving way. Heating systems based on electrical driven heat pumps are the most promising systems available today and the market for these heating systems is fast growing. The combination of heat pumps and solar collectors can potentially offer an even more energy saving technology because the solar collectors can produce most of the domestic hot water and thereby allow the heat pump to mainly produce space heating at lower temperature level with much higher efficiency. In ground heat pump systems, solar collectors can be used to heat up the ground and thereby avoid a gradually decrease of the ground temperature over many heating seasons and thereby decreased efficiency of the heat pump. Nevertheless, how efficient are heat pump systems and solar heat pump systems?

In three large monitoring campaigns in Germany, the performance of nearly 250 traditional air/water and brine/water heat pump systems were measured under real operation conditions. The house types varied from new low energy buildings to older houses with high space heating energy demand. One of the projects "Heat Pumps in Existing Buildings" included heat pump systems in older houses with high space heating demand. The project period was 2008 - 2009. The other two projects "HP Efficiency" and "HP monitor" included heat pump systems in newly built single-family houses. The project periods were 2007 – 2010 and 2012 – 2013 respectively. The seasonal performance factors were defined as useful energy output from the heat pumps divided by the electrical energy consumption of the systems, excluding the electrical consumption of heat distribution pumps and the heat losses in the systems. The seasonal performance factors for the project "Heat Pumps in Existing Buildings" varied from 2.1 to 3.3 with a mean value of 2.6 for air/water heat pumps and from 2.2 to 4.3 with mean value of 3.3 for brine/water heat pumps. For the other two projects, the seasonal performance factors varied from 2.2 to 4.2 with a mean value of 3.1 for air/water heat pumps and from 3.0 to 5.4 with a mean value of 4.0, [1].

Solar heating/heat pump systems were investigated through the International Energy Agency, IEA in a framework between the work programs Solar Heating and Cooling program, Task 44 and the Heat Pump Program, Annex 38 in the period 2010 - 2013. The investigation exposed available system configurations on the international market. A large number of different system configurations were included in the investigations. The system configurations were classified into 7 overall categories and performance factors were defined for solar heating/heat pump systems. In situ measurements in central Europe of 32 air/water and brine/water solar heating/heat pump system under real operation conditions were analyzed within the framework. Among the analyzed systems, the yearly space heating and domestic hot water consumption per m^2 heated floor area varied from 15 to 110 kWh and 4 to 48 kWh respectively. The seasonal performance factors, defined as useful energy output for domestic hot water and space heating consumptions divided by the total electrical energy consumptions varied from 1.3 to 4.8 with a mean value of 3.02, [2].

The company Free Energy markets a hybrid solar heating system, HYSS for single-family houses. The system is prefabricated and comes in a compact cabinet with all components, monitoring equipment and control system. The main components are a domestic hot water tank and a frequency modulated heat pump. The system comes with a user interface, which allows the user to follow the detailed operation of the system. This user interface is accessible at the unit or via a homepage. The system can supply all the energy needed for domestic hot water and space heating in households. The system in combination with a ground storage with horizontal ground source heat exchanger is operated for one year in a laboratory test facility.

The ground storage is designed as patented ASES, Active Solar Energy Storage [3] which store heat in stone dust material. Stone dust is accessible in many regions and has a relatively low cost. The material is compiled of different sized rock particles and may be presented in different compilations. Provided the compilation has a high amount of small particles it will have low porosity. This is essential in a ground storage due to securing good thermal properties as thermal conductivity and heat capacity as well as the smaller particles will protect the collector tubes in the ground storage from damage. [4] When stone dust is compressed it becomes stable and sturdy and it is possible to place a house on top of it.

The aim of the experimental and theoretical investigations is to gain knowledge on the system design, heat- and mass transfer of the system type and the performance figures of the system. The knowledge will be used to assist the manufacturer to improve the system type.

Experimental investigations

Experimental investigations are carried out on a hybrid solar heating system, HYSS with ground storage for a single-family house. The system comprises a 200 l domestic hot water tank, 6.55 m^2 flat plate solar collectors, a 4 kW heat pump and ground storage with length of 10 m, width of 5 m and height of 2 m, corresponding to a total volume of 100 m^3.

The HYSS system

Figure 1 shows a schematic of the experimental setup, consisting of domestic hot water tank, heat pump, solar collectors and ground storage. The figure also shows the measurement points used to control the system (black sensors) and evaluate the energy flows and the performance of the system (orange sensors). Figure 2 shows photos of the solar collector and the HYSS system. Table 1 shows data of the investigated HYSS system.

The solar collector loop and the ground loop are hydraulically connected. The heat transfer fluid is a propylene glycol water mixture. The fluid from the solar collector loop mixes with the fluid from the ground loop before it enters the heat pump evaporator. The solar pump operates with variable speed and the target is to reach an inlet temperature at the heat pump evaporator ≤ 30 °C, both when the heat pump is in operation and during solar energy transfer to the ground storage. During solar energy transfer to the ground storage, a timer restricts the continuous operation time. The purpose is to allow solar energy transfer to the tank, if the conditions are right. The solar pump operates with constant high-volume flow rate during periods with solar energy transfer to the tank. Solar heat is transferred to the tank by circulation of the heat transfer fluid through a coil heat exchanger in the lower part of the tank. The ground pump operates with constant volume flow rate.

Domestic hot water draw off is through a mixing valve located at the top of the domestic hot water tank. Domestic cold water is lead into the bottom of the domestic hot water tank via a pipe leading from the top to the bottom of the tank. The tank, the coils and the cold water pipe are made of stainless steel.

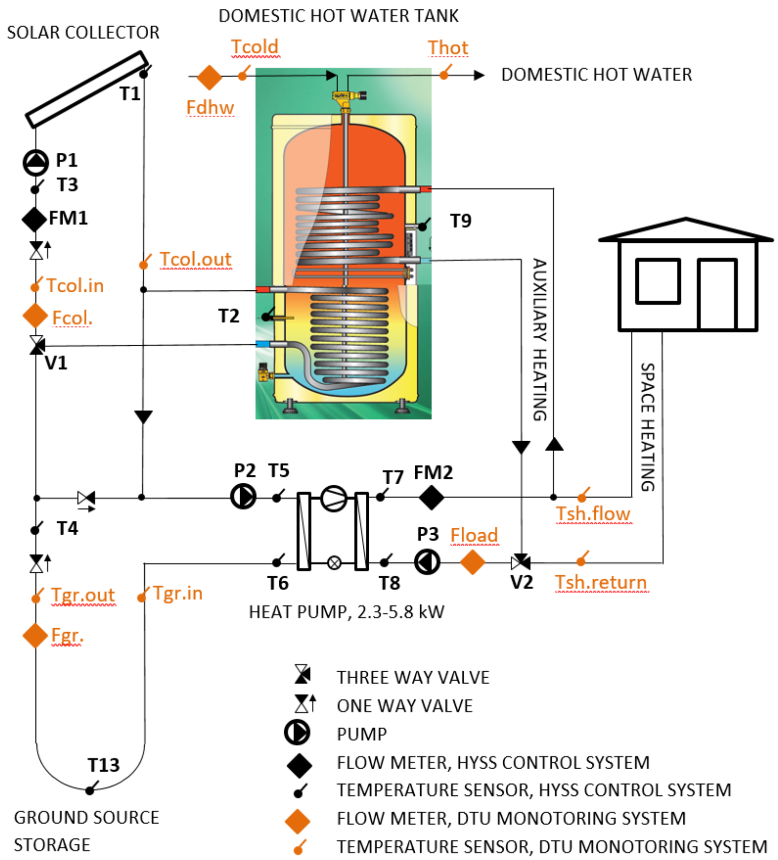

Figure 1. System with measurement sensors.

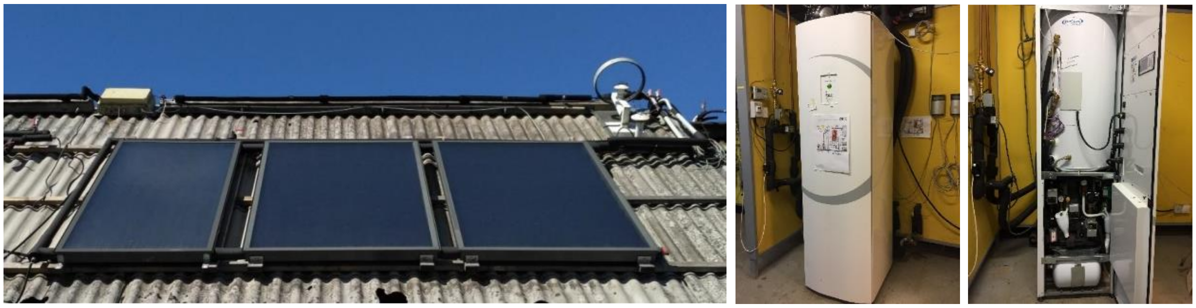

Figure 2. Left: solar collectors. Middle: HYSS system. Right: inside the cabinet of the HYSS system.

Table 1. Data of the investigated HYSS system.

Solar collector area	6.55 m^2
Peak collector efficiency, η_0	0.871
Heat loss coefficient, a_1 / a_2	3.25 $W/m^2/K$ / 0.0172 $W/m^2/K^2$
Efficiency for all incidence angles, η	$\eta_0*k_\Theta-a_1*(T_m-T_a)/G_t-a_2*(T_m-T_a)^2/G_t$
Incidence angle modifier for beam radiation, k_Θ	$1-0.1*S-0.008*S^2$ $S=1/\cos(\Theta)-1$
Collector tilt / Orientation	45° / South
Fluid in solar collector loop and ground loop	35% (weight) propylene glycol/water mixture
Volume flow rate in solar collector loop	0.2 – 1 $l/min/m^2$ collector
Domestic hot water tank volume / auxiliary volume	200 l / 100 l
Inner height / inner diameter of domestic hot water tank	1041 / 492 mm
Surface area of coil heat exchangers in solar collector loop (lower coil) and auxiliary heating loop (upper coil)	0.8 m^2
Heat transfer coefficient of: coil in solar collector loop / coil in auxiliary heating loop	250 W/K / 350 W/K
Relative height of coil in solar collector loop: inlet / outlet	0.42 / 0.09
Relative height of coil in auxiliary heating loop: inlet / outlet	0.77 / 0.5
Relative height of temperature sensor to control solar collector loop	0.3
Relative height of temperature sensor to control auxiliary heating loop	0.64
Insulation material of domestic hot water tank / thermal conductivity	ECO foam / 0.025 W/m/K
Insulation thickness for domestic hot water tank: top / side / bottom	50 / 40 / 50 mm
Heat loss coefficient of domestic hot water tank: theoretical / measured	1.22 W/K / 5.62 W/K
Heat pump capacity / type	4 kW heat pump, single stage brine/water
Heat pump capacity with frequency inverter, 30 – 70 Hz	2.3 – 5.8 kW

Maximum inlet temperature on source side	43 °C
Refrigerant	R410a
Power consumption of pump in solar collector loop	21.5 W
Power consumption of pump in ground loop	83 W
Power consumption of pump in heat distribution loops	45.5 W

The ground storage

Figure 3 shows a schematic layout of the ground storage and the location of temperature sensors in the ground and Figure 4 shows photos of the ground storage during construction. The soil composition in and around the ground source storage and data of the ground source storage can be seen in Table 2.

TS1 measures the temperatures next to the ground storage and serve as a reference for the temperatures in the undisturbed ground. TS4 measure the ground temperature under the insulation next to the storage and TS2 and TS3 measures the temperatures in the ground storage. T13 is used to control the operation of solar energy to ground.

The ground source heat exchanger has two parallel loops, shown with blue and red color in Figure 3. The flow direction in the loops is the same whether the heat pump uses heat from the storage or the solar collectors feed heat into the storage. The two loops are identical and it is assumed that the flow is equally distributed in the two identical loops.

The ground source tubes lie 3 m below the soil surface in a layer of compressed stone dust. On top of the compressed stone dust layer, there is a layer of compressed boulder clay. On top of the compressed soil, there is top insulation and finally topsoil and grass. The top insulation covers a larger area than the area of the ground source storage, in order to reduce the heat loss of the ground source storage further. There is also a vertical side insulation layer. The reason for the vertical side insulation layer is to separate the ground source storage from a neighboring ground source heat exchanger, which has ground tubes 1 m below the soil surface. The side insulation layer stretches from the top of the ground source storage to 1 m below the ground source storage.

Feeding tubes connect the ground source storage to the HYSS system in the indoor test facility. The feeding tubes are insulated and lie 1 m below the soil surface.

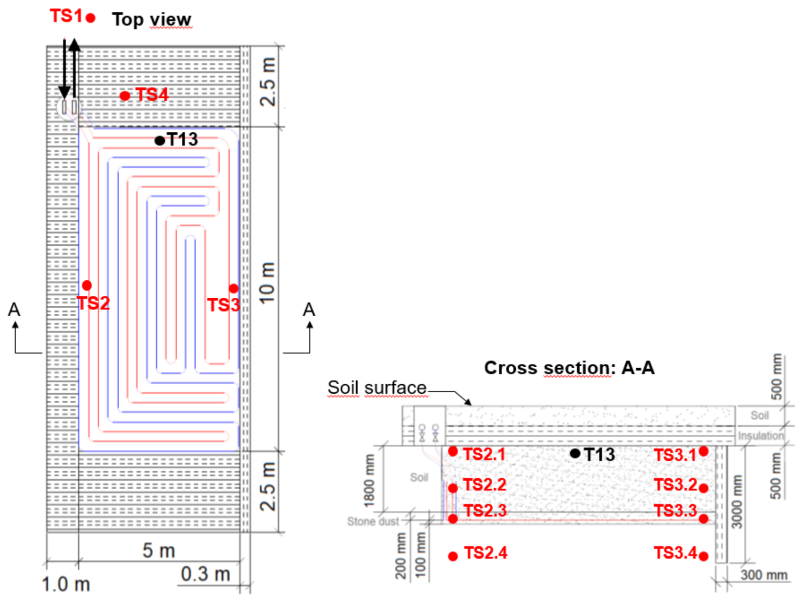

Figure 3. Ground storage layout with measurement sensors.

Figure 4. Pictures of ground storage during construction.

Table 2. Ground storage data.

Soil composition in undisturbed ground, next to ground storage. Depth below soil surface. 0 m correspond to soil surface.	0 – 1.6 m	:	Mulch, sandy, clay, black
	1.6 – 3.2 m	:	Clay, fat, sandy, brown
	3.2 – 7.8 m	:	Sand, fine-grained, brown
	7.8 – 10 m	:	Sand, fine-grained, silty, brown
	>15 m	:	Ground water
Soil composition in ground storage. Depth below soil surface. 0 m correspond to soil surface.	1 – 2.8 m	:	Clay, fat, sandy, brown
	2.8 – 3 m	:	Stone dust (particle size: 0-3 mm)
Location of temperature sensors in ground below soil surface. 0 m correspond to soil surface. X refers to sensor number 1, 2, 3 and 4 in Figure 3.	TSX.1	:	1.1 m
	TSX.2	:	2 m
	TSX.3	:	2.9 m
	TSX.4	:	4 m
Insulation material / thermal conductivity	Jackopor 60, expanded polystyrene (EPS)		

	/ 0.041 W/m/K
Thickness of top insulation	500 mm
Thickness of side insulation	300 mm
Ground tubes and feeding tubes, material	Polyethylene, PE 80
Diameter of ground tubes, outer / inner	25 / 21 mm
Length per ground loop / total length of ground loop	80 / 160 m
Distance between ground tubes	300 mm
Diameter of feeding tubes, outer / inner	40 / 35.2 mm
Distance between ground storage and HYSS system	36 m

Measurement equipment

The sensors used to measure the temperatures and energy flows of HYSS are listed in Table 3.

Table 3. Measurement equipment.

Equipment	Type	Location	Accuracy
Flow sensor	Brunata HGQ1-R0-184	Ground loop	± 1 %
	Brunata HGQ1-R0-184	Solar collector loop	± 2 %
	Kamstrup 602	SH loop	± 1 %
	Clorius Combimeter 1.5 EPD	DHW loop	± 2 %
Temperature sensor	Copper/constantan, type TT		± 0.5 K
Energy meter	Malmbergs 09 815 52	Total	± 0.5 %

The energy quantities in the loops are determined from measured temperatures and volume flow rates and it is estimated that the accuracy of the measured energy quantities are within 5 %. The electricity consumption is measured with energy meters and it is estimated that the accuracy of the measured electrical energy quantities are within 0.5 %.

Test period and test conditions

The test period is one year, from November 2018 to October 2019.

Equal portions of domestic hot water are tapped three times a day in the morning, at noon and in the evening. In total, an energy amount 4.5 kWh is tapped every day. The yearly hot water consumption is 1640 kWh. This corresponds to a daily hot water consumption of 100 litres heated from 10 °C to 50 °C. The volume flow rate during tapping is around 4 l/min.

The space heating consumption drawn from the system is about 2200 kWh corresponding to a space heating consumption of a single-family house of 140 m^2 with space heating demand of 16 $kWh/m^2/year$.

The control strategy for the circulation pump, P3 in the heat distribution system is that the pump is in continuous operation during the heating season. When the measured temperature difference between the condenser outlet temperature and inlet temperature is larger than 3 K, the heat pump turns on for space heating production. Whenever the set point temperature in the domestic hot water tank drops below the threshold value, the valve V2 switches and the heat pump produces hot water for the domestic hot water tank.

Average daily solar radiation on collector, average daily ambient temperature and monthly energy consumption for domestic hot water and space heating can be seen in Figure 5. Due to malfunction of a valve, the space heating consumption is not on in October as intended.

Figure 5. Measured weather data and energy drawn from HYSS in test period. Left: Solar radiation on solar collector and average ambient temperature. Right: Space heating and domestic hot water consumption.

Control strategy of HYSS can be seen in Table 4.

Table 4. Control strategy of HYSS.

Solar to heat pump	1. priority
Volume flow rate in solar collector loop (variable speed pump)	0.2 – 1 l/min/m^2 collector
Volume flow rate in ground loop	12 l/min
Maximum inlet temperature to heat pump resulting from mixing of volume flow rate from solar collector loop with volume flow rate from ground loop mixed	≤ 30 °C
Solar to tank	2. priority
Volume flow rate in solar collector loop	1 l/min/m^2 collector
Start temperature conditions	T1 > T2 + 5 K and T2 < 70 °C
Stop temperature conditions	T1 < T2 + 2 K
Solar to ground	3. priority
Volume flow rate in solar collector loop (variable speed pump)	0.2 – 1 l/min/m^2 collector
Volume flow rate in ground loop	12 l/min
Maximum inlet temperature to heat pump resulting from mixing of volume flow rate from solar collector loop with volume flow rate from ground loop mixed	≤ 30 °C
Timer, max. continuous runtime / stop time	15 min / 2 min
Start temperature conditions	T1 > T13 + 8 K
Stop temperature conditions	T1 < T13 + 5 K

Heat pump to tank	1. priority (domestic hot water production)
Volume flow rate in heat pump tank loop	15 l/min
Volume flow rate in ground loop	12 l/min
Set point temperature in tank (T9set)	52 °C
Start temperature conditions	T9 < 52 °C – 4 K
Stop temperature conditions	T9 > 52 °C
Heat pump to space heating	2. priority
Volume flow rate in heat pump space heating loop	7 l/min
Volume flow rate in ground loop	12 l/min
Set point temperature in tank (T7set)	28 °C
Start temperature conditions	**$\Delta_{T7-T8} \geq 3$ K**
Stop temperature conditions	**$\Delta_{T7-T8} < 3$ K**

Test results

Figure 6 shows monthly energy flows and the energy consumption of circulation pumps in the solar heating/heat pump system in the test period. The energy consumption of the circulation pump in the heat distribution system, P3 is relatively high and the reason is that the pump has been running all year, also in the summer period where it should only work during hot water production for the domestic hot water tank.

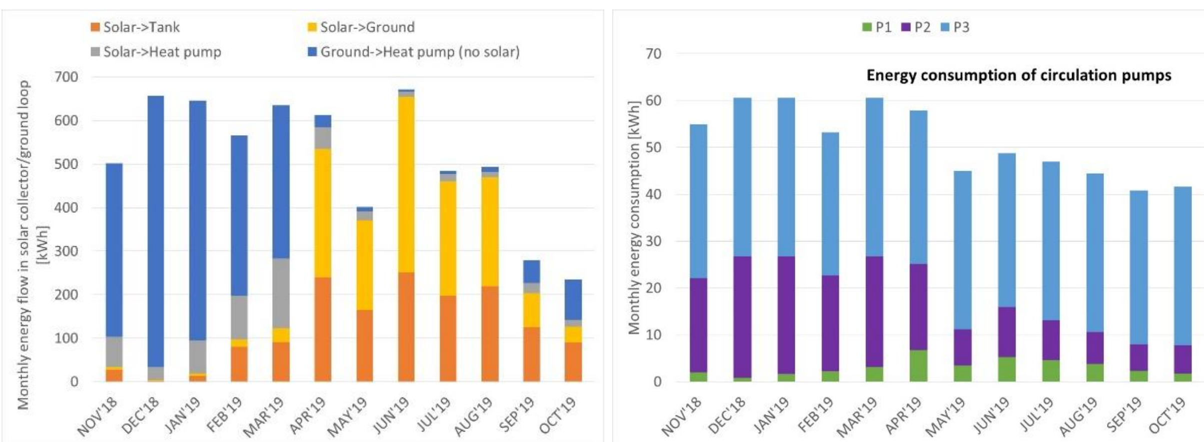

Figure 6. Measured daily energy flows and energy consumption of circulation pumps in HYSS.

Figure 7 shows a hydraulic layout of HYSS and a graphical definition of seasonal performance factors, SPF. The analytical definition of the performance factors is found in equation (1) – (4), [2].

The seasonal performance factor expresses the ratio between the useful energy output and the energy input. The seasonal performance factors are defined for a period, e.g. month or year.

As it shows, there are many ways to define the seasonal performance factor. It is therefore most important to use the same definition when comparing the seasonal performance factors for different systems. However, in order to have a completely fair comparison of the seasonal performance factors for different heating systems, all heat losses and the total electricity consumption should be included. The seasonal performance factors described by equation (1) – (3) do not include heat losses and all the electricity consumptions of the system. Only the seasonal performance factor described by equation (4) includes all heat losses and the total electricity consumption of the system.

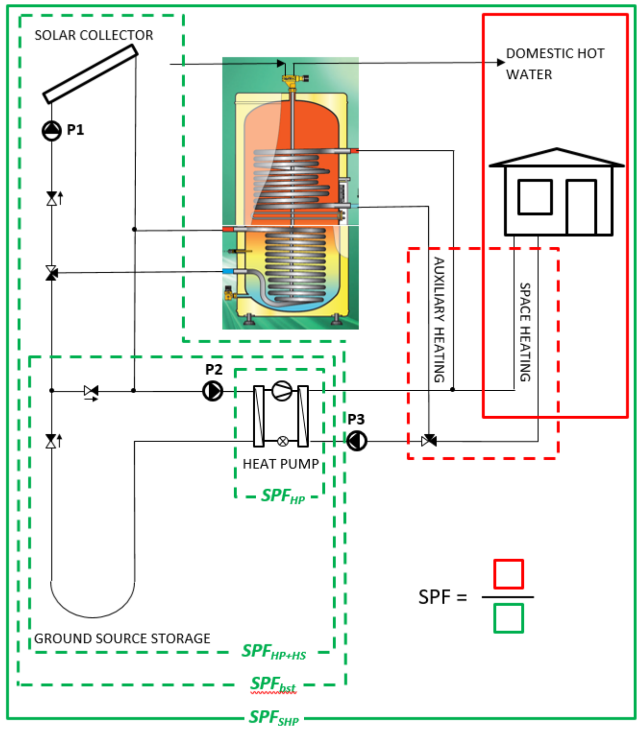

Figure 7. Graphical definition of seasonal performance factors, SPF.

$$SPF_{HP} = \frac{\sum Q_{HP}}{\sum(E_{HP} + E_{ctr})} \quad (1)$$

$$SPF_{HP+HS} = \frac{\sum Q_{HP}}{\sum(E_{HP} + E_{ctr} + E_{CPHS})} \quad (2)$$

$$SPF_{bst} = \frac{\sum(Q_{HP} + Q_{Solar})}{\sum(E_{HP} + E_{ctr} + E_{CPHS} + E_{CPSolar})} \quad (3)$$

$$SPF_{SHP} = \frac{\sum(Q_{DHW} + Q_{SH})}{\sum(E_{HP} + E_{ctr} + E_{CPHS} + E_{CPDist} + E_{CPSolar})} \quad (4)$$

Figure 8 shows monthly and yearly seasonal performance factors determined by equation (4).

It is not possible to determine the other seasonal performance factors described by equation (1) – (3), because the heating power of the heat pump is not measured.

The measured seasonal performance factors to the left in Figure 8 are relatively low and one reason for this is the continuous operation during the whole year of the heat distribution pump, P3 in the heat distribution loop. Therefore, energy consumption for the heat distribution pump, P3 is subtracted in the period from April to September where it was not supposed to be in operation. Further, the seasonal performance factors are determined under the assumption that the heat distribution pump, P3 is only in operation during domestic hot water and space heating production. The improved seasonal performance factors are seen in Figure 8, middle and right respectively.

The measured seasonal performance factors show high sensitivity to malfunction in the system operation.

The measured seasonal performance factors all lie within the range of previous in-situ measured solar heat pump systems, [2]. The measured seasonal performance factors do not compare directly to the previous in-situ measured heat pump system performances because there only SPF_{bst} are given, [1].

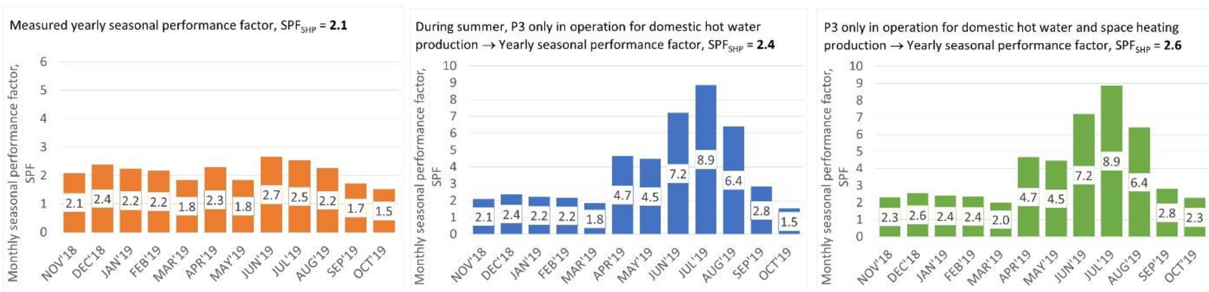

Figure 8. Measured monthly and yearly seasonal performance factors for HYSS.

Figure 9 shows average daily measured ground temperatures. The figures also show the daily average temperature and solar radiation on horizontal. Figure 10 shows the temperature difference in the ground from November 1, 2018 to October 31, 2019. It can be seen that temperature increase during 1 year around 1 degree in the storage in level of the ground tubes. The other storage temperatures are all lower exactly 1 year later. Further, there is no space heating consumption in October due to malfunction of a valve. With space heating consumption in October, the storage temperatures would have been lower than they are now. This indicates that the solar collector area is too small for the storage size with the domestic hot water and space heating consumption applied for the HYSS in the test period.

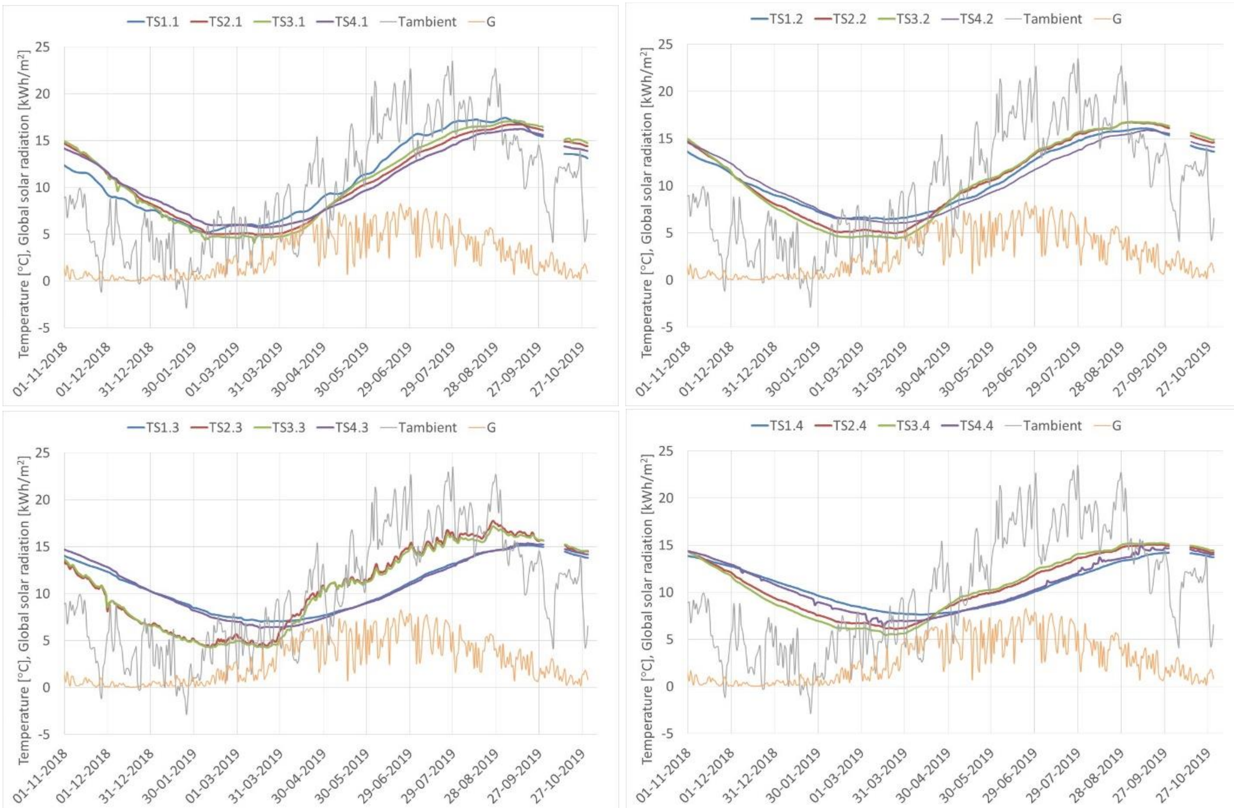

Figure 9. Measured average daily temperatures and global solar radiation.

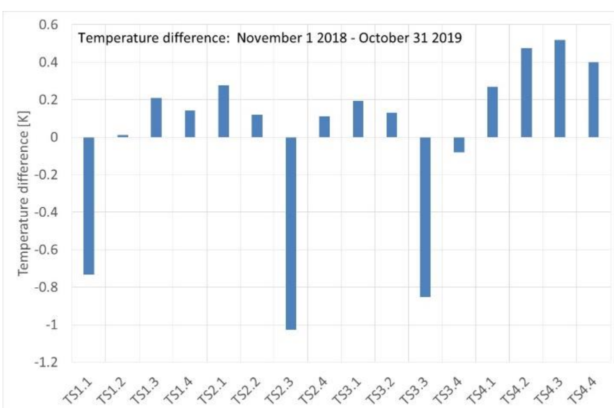

Figure 10. Measured temperature difference in ground.

Figure 11 shows the power transfer in the ground storage in periods with the heat pump in operation without solar assistance and in periods where solar energy is transferred to the ground. The power transfer is shown as function of the inlet temperature to the ground storage.

The figures show measurements from the months November 2018, March 2019, June 2019 and October 2019.

It is clear to see that both fluid inlet temperature and power transferred from the ground storage to the fluid with heat pump alone operation are much lower than fluid inlet temperature and power transfer to the ground storage with solar to ground operation. The power uptake from the ground storage to the fluid is 10 – 20 W/m while power transfer to the ground storage is 10 – 180 W/m.

One reason for this difference is the larger temperature difference, which increases the heat transfer when solar is transferred to the ground. Further, the ground tubes are made of polymer, which has a large thermal expansion coefficient. The thermal expansion may result in a better contact to the ground in periods with solar to ground operation due to higher fluid inlet temperatures and thermal contraction may result in a worse contact to the ground due to lower fluid inlet temperatures in periods with heat pump alone operation.

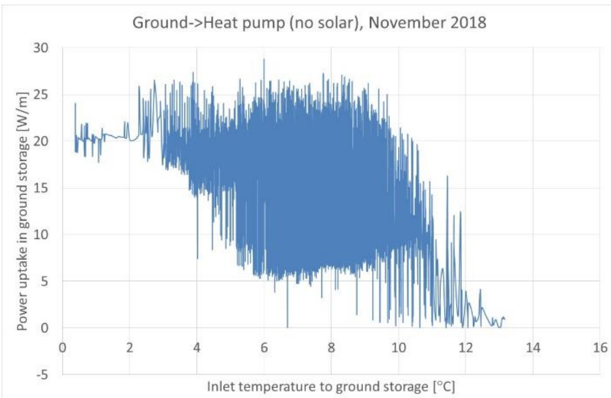

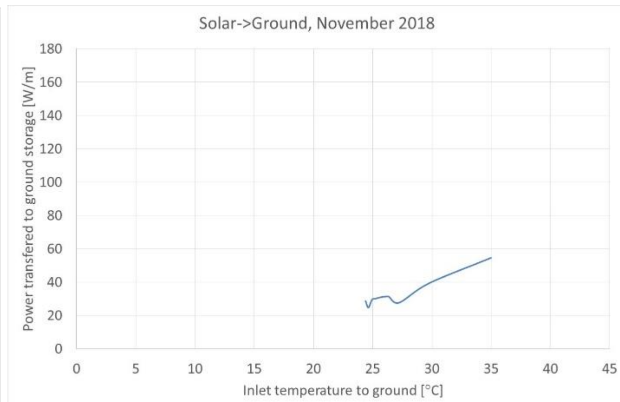

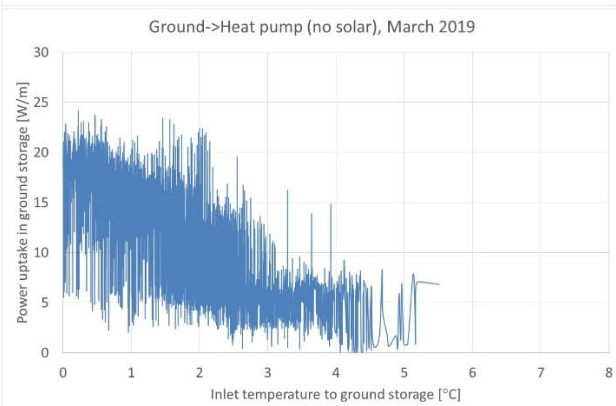

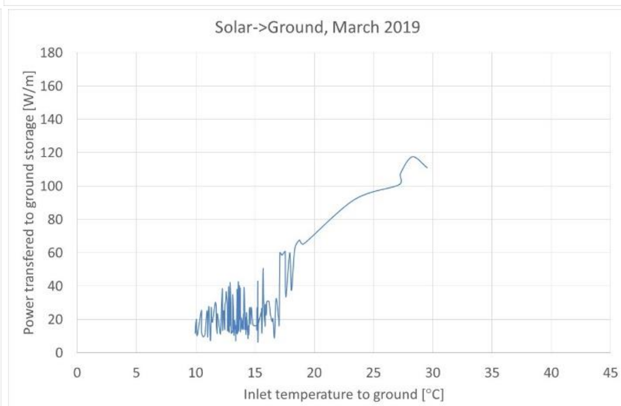

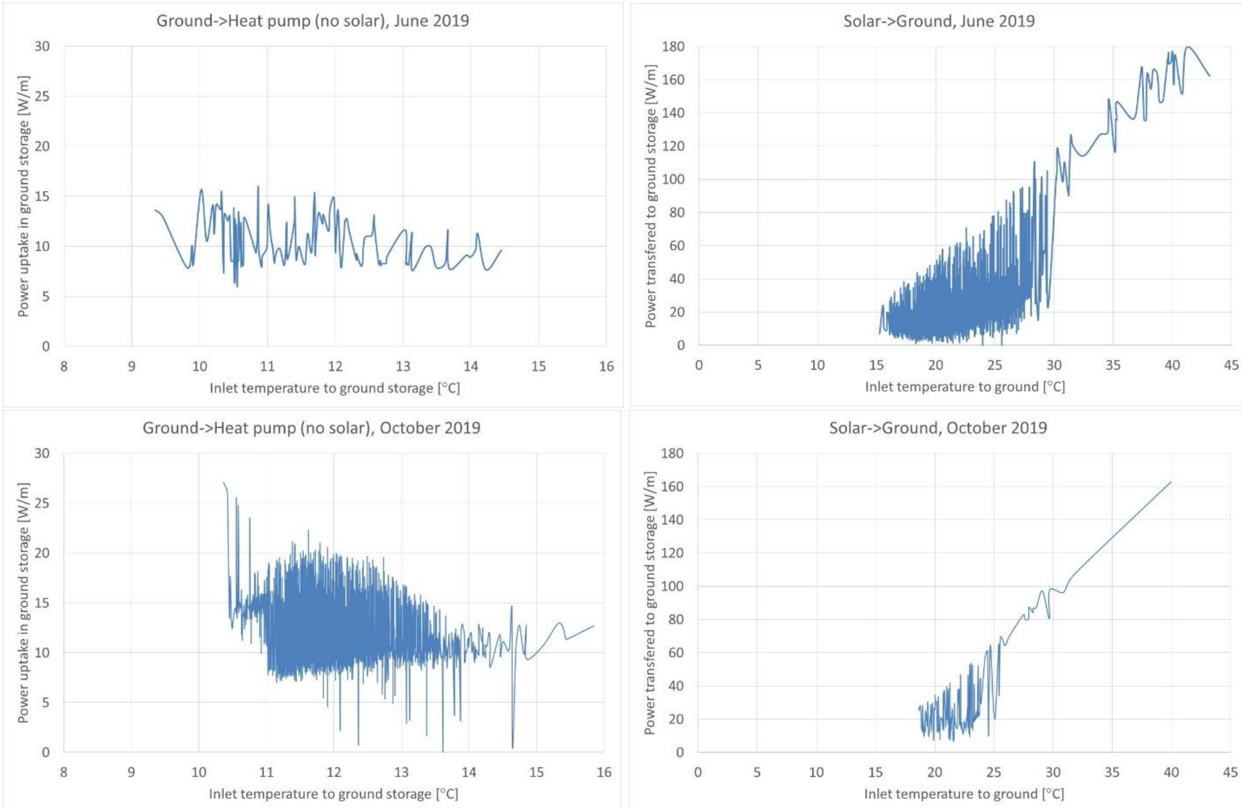

Figure 11. Measured power uptake in ground storage and power transfer to ground storage.

Theoretical investigations

The numerical model

A numerical simulation model of HYSS with ground storage is built in TRNSYS. Figure 12 shows the graphical layout of the numerical simulation model of HYSS.

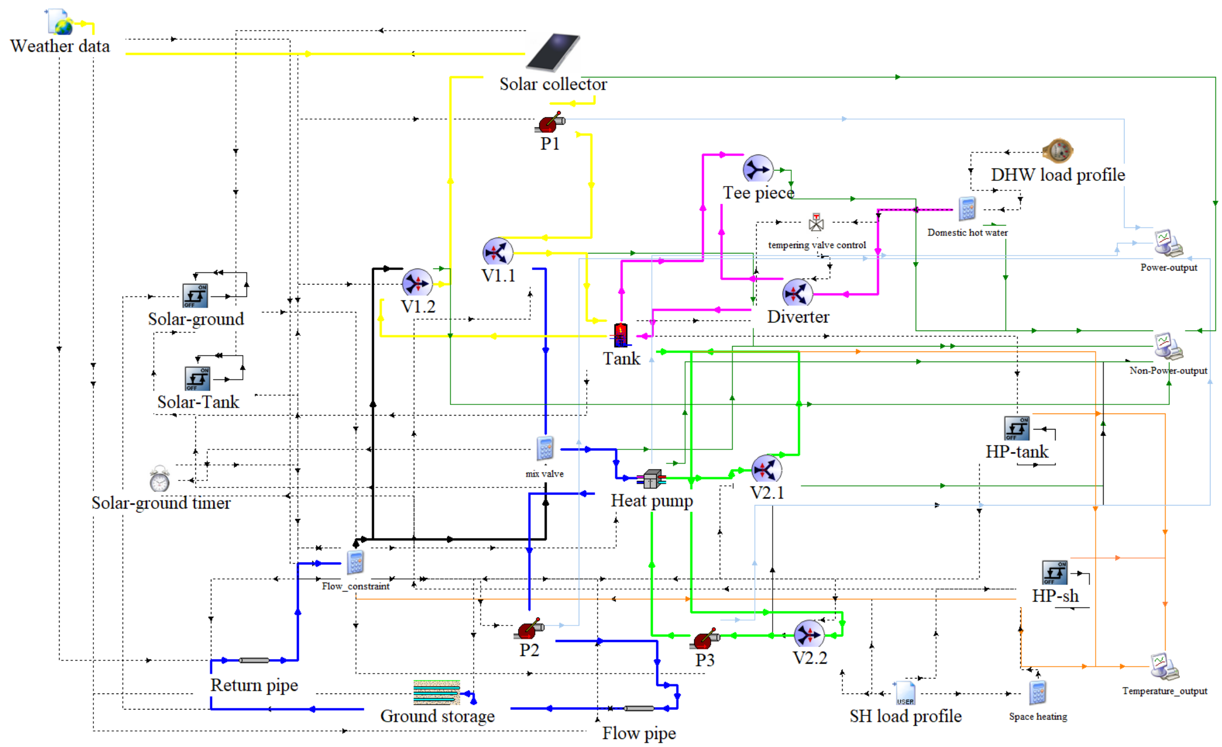

Figure 12. The numerical model of HYSS in TRNSYS.

Inputs for the simulation model are described in the tables and the text in previous sections.

Input for the ground model is described in Table 5. The start temperature profile for the boundary ground surface is described by the Kusuda correlation for soil temperatures [5]. In Figure 13 temperature profiles for the boundary surface next to the ground storage are shown. The figure, also shows measured temperatures in the ground from a 10 m deep borehole with temperature measurements every meter. The 10 m deep borehole is located only 20 m away from the ground storage and these measurements are used to set the parameters for the Kusuda correlation. Although, not all calculated months fit the measured months perfectly, the calculated temperatures fit very well to the measured temperatures both in the deep earth temperature and in the amplitude of the surface temperature.

Table 5. Input for the ground model.

Number of pipes in layer	20
Number of pipe layers	1
Number of soil layers	1
Nodes along the pipe axis	4
Pipe length	10 m
Pipe thermal conductivity	0.35 W/m/K
Pipe/soil resistance	0.27 - 0.45 m^2K/W
Horizontal pipe separation between centerlines	0.24 m
R-value for surface insulation	12.2 m^2K/W
Far field distance for side wall insulation / boundary mode	1 m / Adiabatic

Far field distance for other sides /boundary mode	10 m / Conductive
Fluid specific heat	3818 J/kg/K
Fluid density	1033 kg/m^3
Fluid thermal conductivity	0.42 W/m/K
Fluid viscosity	0.005 kg/m/s
Thermal conductivity of soil layer	2.9 W/m/K
Density of soil layer	1800 kg/m^3
Specific heat of soil layer	1200 J/kg/K
Deep earth (average surface) temperature	11.1 °C
Amplitude of surface temperature	9 K
Smallest node size	0.125 m
Nodal size multiplier	2

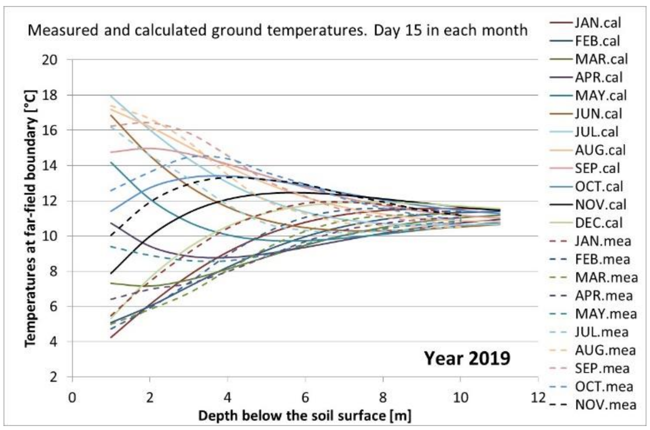

Figure 13. Kusuda correlation for boundary soil temperature and measured boundary soil temperatures.

The heat pump is simulated with a performance map and the parameters of heating power from the condenser and the power consumption of the compressor are shown in Figure 14. The heat pump is operated with a frequency inverter, but such a component is not available in TRNSYS at present. The shown performance map is fitted with measured energy quantities.

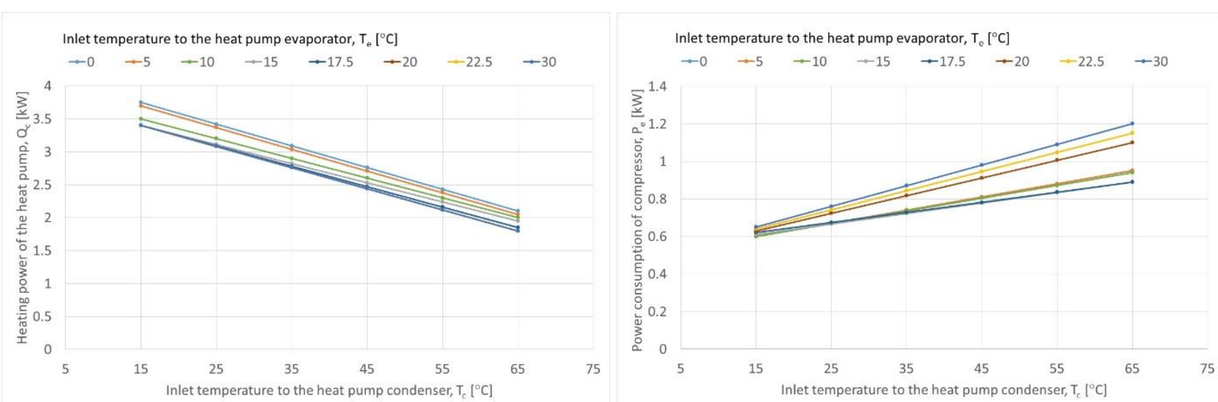

Figure 14. Heat pump heating power and power consumption.

Validation of the numerical model

The numerical model simulation model is validated against measured daily energy quantities.

The energy quantities are: Electrical energy consumption by heat pump, energy absorbed by heat pump, energy delivered to system by heat pump, energy delivered by solar collector to system, solar energy delivered to domestic hot water tank, solar energy delivered to heat pump, solar energy delivered to ground, energy to space heating, auxiliary energy to domestic hot water tank and energy for domestic hot water tapped from the domestic hot water tank.

The months of March and June are used for the validation. In March, the system delivers energy for both space heating and domestic hot water and in June, the system only delivers energy for domestic hot water.

Figure 15 shows the daily measured and calculated energy quantities. There is a good degree of similarity between measured and calculated energy quantities.

In Table 6 the most important energy quantities are summed for the whole measurement period, except the first day, which is considered as adaptation day for the calculations. The differences between the measured and the calculated energy quantities are clearly within the measurement accuracy of the measured energy quantities.

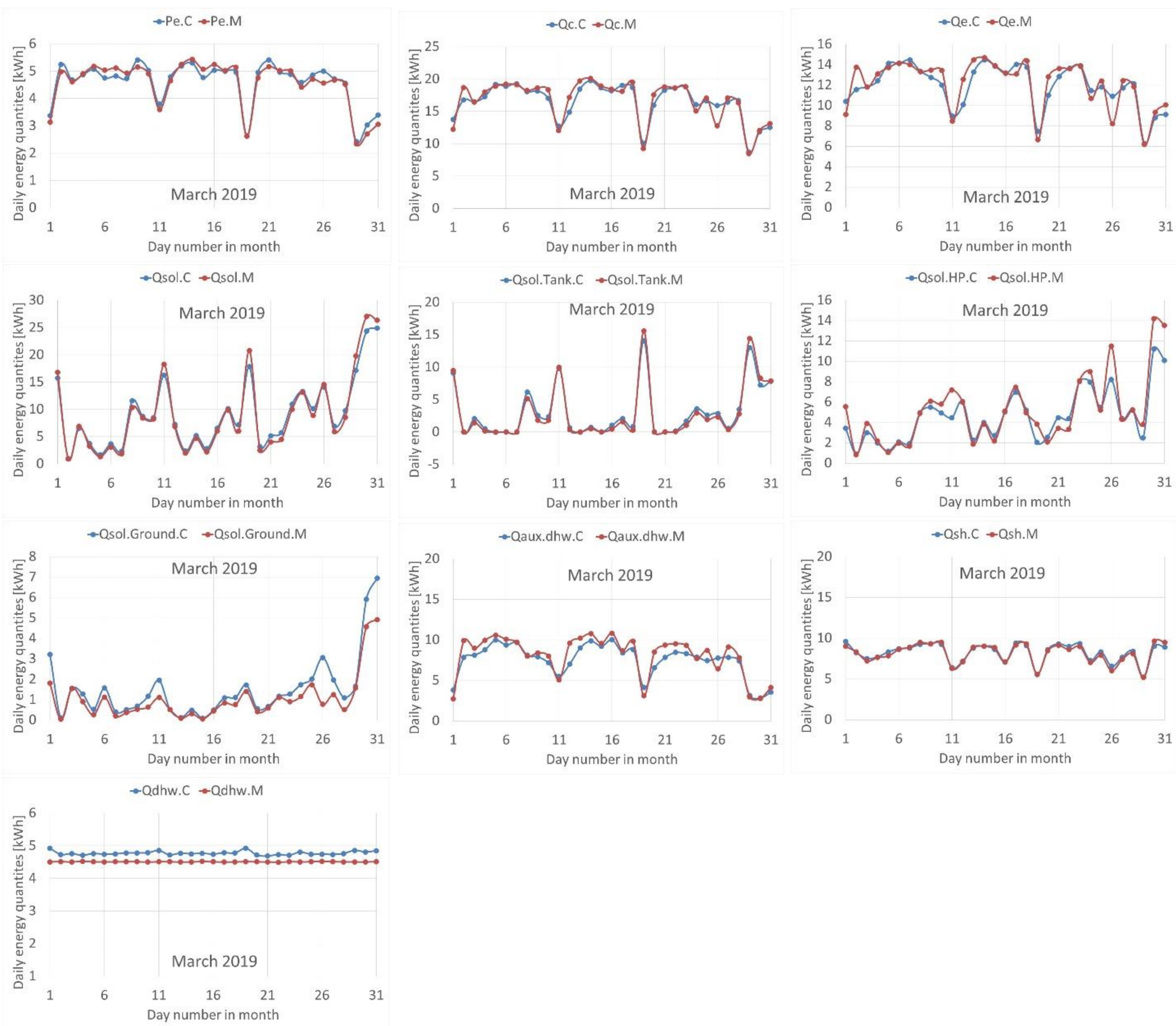

Figure 15. Daily energy quantities in March 2019, measured and calculated.

Table 6. Summed energy quantities in March 2019, measured and calculated.

Period: March 2 - 31	Electrical energy consumed by heat pump, P_e [kWh]	Energy absorbed by heat pump, Q_e [kWh]	Energy delivered to system by heat pump, Q_c [kWh]	Space heating and domestic hot water consumption kWh]
Measured	138	367	505	379
Calculated	139	359	498	389
Difference [%]	-0.7	2.2	1.4	-2.6

Figure 16 shows the daily measured and calculated energy quantities in June 2019. There is a good degree of similarity between measured and calculated energy quantities.

In Table 7, the important energy quantities are summed for the whole measurement period in June 2019, except the first day, which is considered as adaptation day for the calculations. The differences between the measured and the calculated energy quantities are clearly within the measurement accuracy on the measured energy quantities.

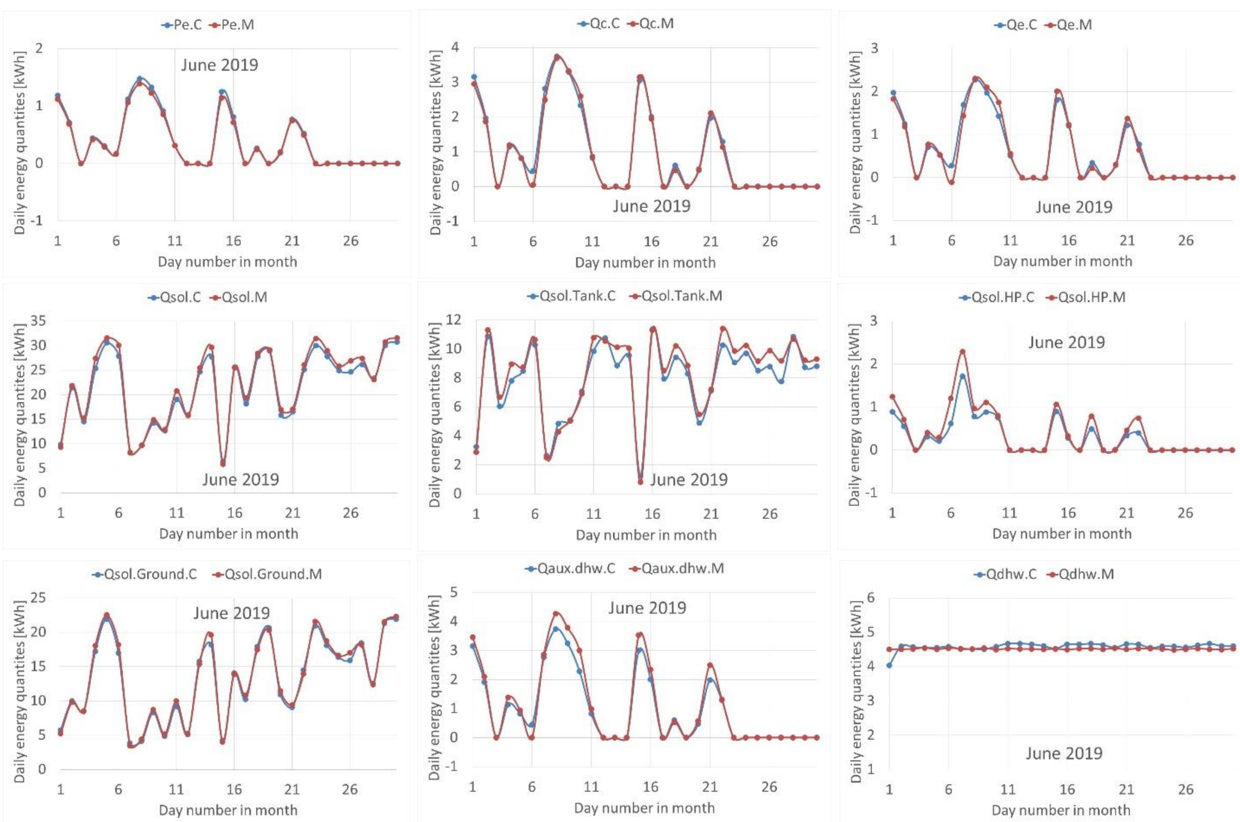

Figure 16. Daily energy quantities in June 2019, measured and calculated.

Table 7. Summed energy quantities in June 2019, measured and calculated.

Period: June 2 - 30	Electrical energy consumed by heat pump, P_e [kWh]	Energy absorbed by heat pump, Q_e [kWh]	Energy delivered to system by heat pump, Q_c [kWh]	Domestic hot water consumption kWh]
Measured	9.9	16	26	131
Calculated	10.6	16	27	133
Difference [%]	-7.1	0	-3.8	-1.5

Calculation with the numerical model

Yearly performances of HYSS are calculated with the validated simulation model with solar collector areas of 6.55 m^2 and 13.5 m^2 and weather data from the Danish design reference year, DRY.

Figure 17 shows the average daily solar radiation on the solar collector, average daily ambient temperature with DRY. The figure also shows the monthly energy consumption for domestic hot water and space heating.

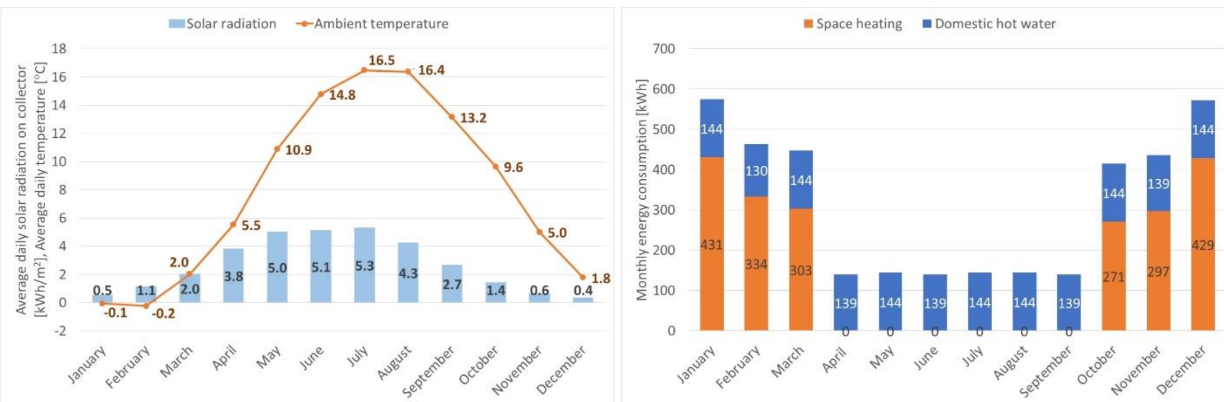

Figure 17. Weather data from DRY and calculated energy drawn from model of HYSS. Left: Solar radiation on solar collector and average ambient temperature. Right: Space heating and domestic hot water consumption.

Calculated yearly performance of HYSS with solar collector area of 6.55 m^2

Figure 18 shows the calculated monthly energy flows and the energy consumption of circulation pumps.

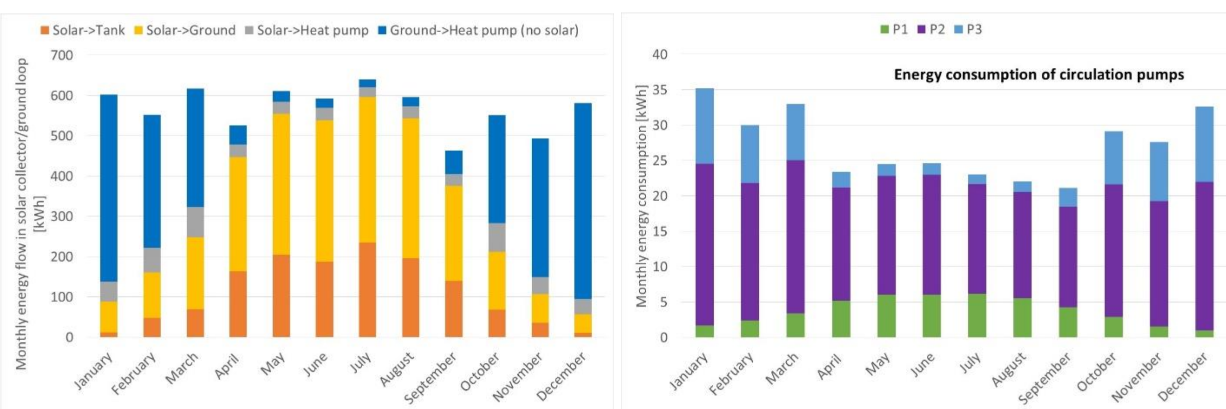

Figure 18. Calculated daily energy flows and energy consumption of circulation pumps in numerical model of HYSS with solar collector area of 6.55 m^2.

Figure 19 shows daily, monthly and yearly seasonal performance factors calculated by equation (1) – (4). The energy consumption of circulation pumps is only included if the pumps are in operation with a purpose. Calculation of the yearly seasonal performance factor, SPF_{SHP} with P3 in continuous operation through the whole year gives SPF_{SHP} of 2.1, which fits the measured SPF_{SHP}.

The seasonal performance factors vary through the year, especially on a daily bases and especially the performance factor, SPF_{bst} described by equation (3). For SPF_{bst} a very well insulated system with low tank heat losses will reduce the seasonal performance factor while a poor insulated system with high tank heat losses will increase the seasonal performance factor.

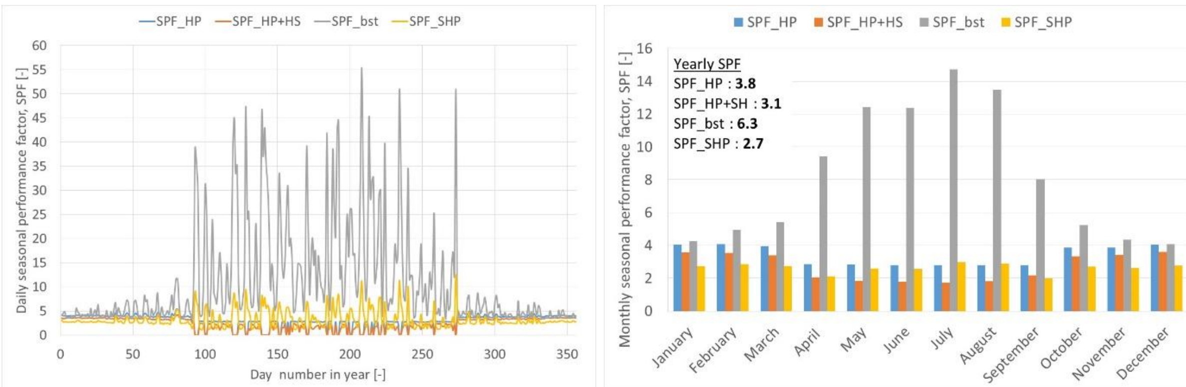

Figure 19. Measured seasonal performance factors for HYSS with solar collector area of 6.55 m².

Calculated yearly performance of HYSS with solar collector area of 13.1 m²

Figure 20 shows the calculated monthly energy flows and the energy consumption of circulation pumps.

It can be seen that solar energy quantities increase and the energy quantities drawn from the ground during heat pump alone operation decrease. Especially, the amount of solar energy transferred to the tank increases with the larger solar collector area. The increase of solar energy to the ground storage is limited by the volume flow rate in the ground loop and the inlet temperature to the ground, which are the same as in the calculations with the smaller solar collector area.

The energy consumption of the circulation pump in the heat distribution loop, P3 decreases when the solar collector area increases from 6.55 m² to 13.1 m² because the solar collectors produce a larger part of the energy in domestic hot water tank.

The energy consumption of the circulation pump in the ground loop, P2 decreases when the solar collector area increases from 6.55 m² to 13.1 m² because the operation time of the heat pump and the circulation pump in the solar collector solar loop, P1 decreases.

The energy consumptions of the circulation pump in the solar collector loop, P1 is almost the same with solar collector areas of 6.55 m² and 13.1 m² because the maximum temperatures in the tank and to the ground are reached faster.

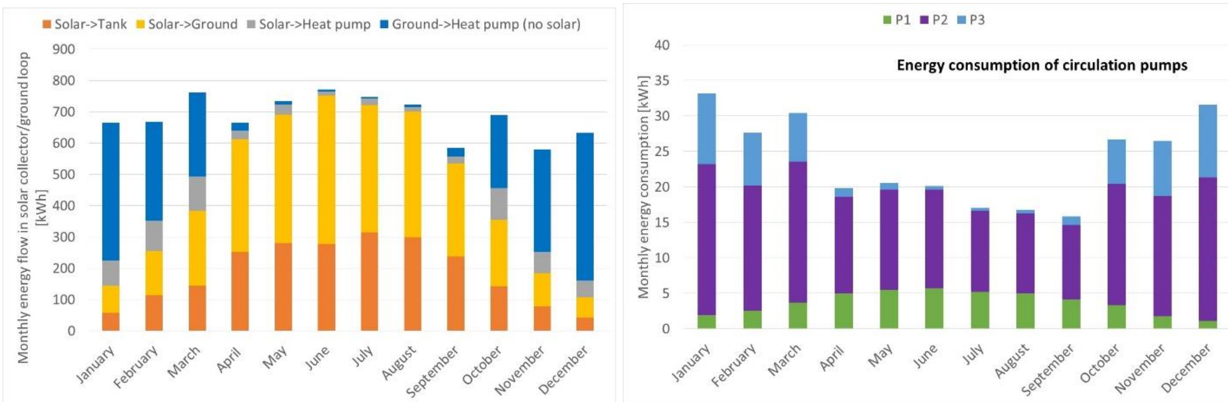

Figure 20. Calculated daily energy flows and energy consumption of circulation pumps in numerical model of HYSS with solar collector area of 13.1 m^2.

Figure 21 shows daily, monthly and yearly seasonal performance factors calculated by equation (1) – (4). The energy consumption of circulation pumps is only included if the pumps are in operation with a purpose.

The seasonal performance factors vary through the year, especially on a daily basis and especially the performance factor, SPF_{bst} described by equation (3), which leave out the heat losses in the system.

All the seasonal performance factors increase because of the increased solar collector area. The seasonal performance factors SPF_{HP} and SPF_{HP+HS} described by equation (1) and (2) are not very influenced by the solar collectors and increase only slightly because the heat pump produces less domestic hot water at high temperature with low heat pump efficiency. The increased solar energy transfer to the system increases the temperature level in the system and thereby the heat loss of the system. Hence, the seasonal performance factor SPF_{bst}, which does not include the coverage of heat losses in the system increases dramatically with the enlarged solar collector area.

The increase of the seasonal performance factor SPF_{SHP} is due to the reduced operation of the heat pump for domestic hot water production. Consequently, a good way to increase the overall seasonal performance factor SPF_{SHP} further is to reduce the heat loss of the domestic hot water tank.

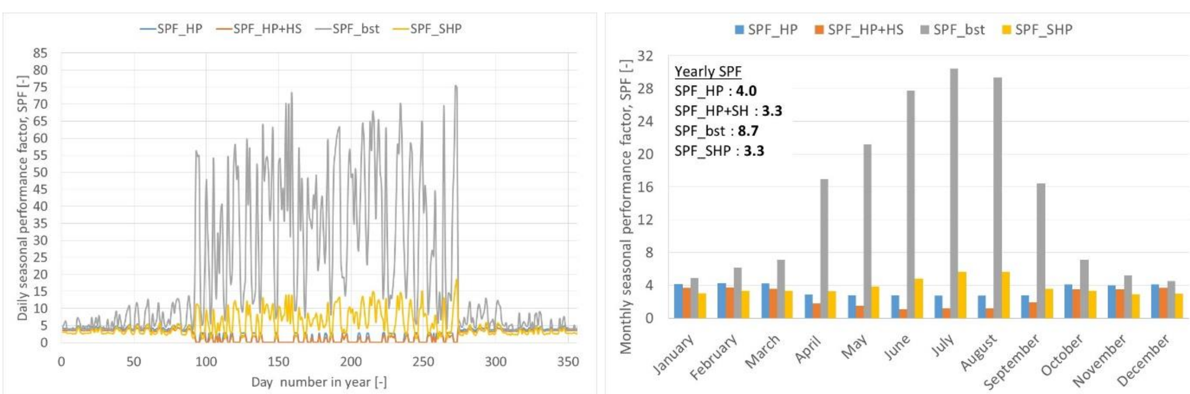

Figure 21. Measured seasonal performance factors for HYSS with solar collector area of 13.1 m^2.

Calculated yearly performance of HYSS with solar collector area of 6.55 m^2 and reduced heat loss of the domestic hot water tank

The heat loss coefficient of the tank is reduced from the measured value of 5.62 W/K to the theoretically calculated heat loss coefficient of 1.22 W/K. Figure 22 shows the calculated monthly energy flows and the energy consumption of circulation pumps.

It can be seen that solar energy quantities decrease to the tank and the heat pump while the solar energy quantities to the ground storage increase compared to the calculations with solar collector area of 6.55 m^2 and the measured heat loss coefficient of 5.62 W/K. Also the energy drawn from the ground by the heat pump and the energy consumption of P3 decreases.

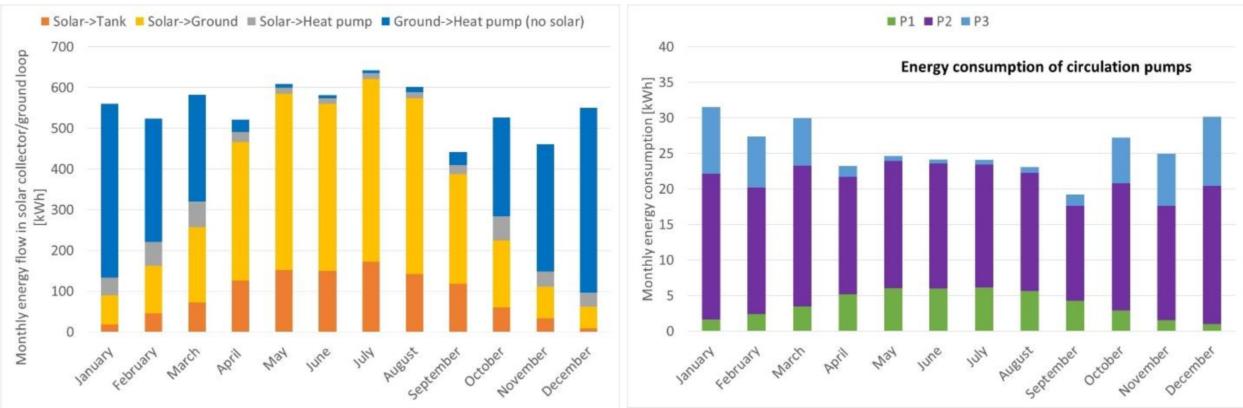

Figure 22. Calculated daily energy flows and energy consumption of circulation pumps in numerical model of HYSS with solar collector area of 6.55 m^{2}and tank heat loss coefficient of 1.22 W/K.

Figure 23 shows daily, monthly and yearly seasonal performance factors calculated by equation (1) – (4). The energy consumption of circulation pumps is only included if the pumps are in operation with a purpose.

All the seasonal performance factors increase due of the decreased heat loss of the domestic hot water tank. Further, the seasonal performance factors are very similar to the seasonal performance factors calculated with the numerical model with 13.1 m^2 and the measured heat loss coefficient of the tank of 5.62 W/K.

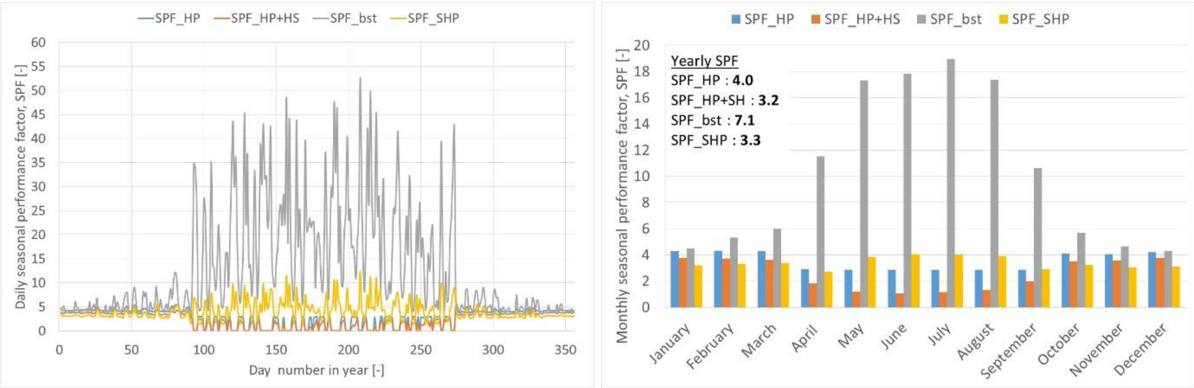

Figure 23. Measured seasonal performance factors for HYSS with solar collector area of 6.55 m^{2}and tank heat loss coefficient of 1.22 W/K.

The results clearly show the importance of well-insulated components. Further, well-insulated system components are the most cost-effective way to reach high system efficiencies.

Conclusion

A marketed hybrid solar heating system with ground storage for single-family houses is investigated experimentally and theoretically. The experimental investigations are carried out in a laboratory test facility where the system has been installed and operation for 1 year from November 2018 to October 2019. Temperatures, volume flow rates and electric energy consumption are measured allowing detailed determination of energy flows in the system. A numerical model of the system is built in TRNSYS and validated against the measurements. The validated numerical model is used to calculate the yearly thermal performance of the system and to perform parameter variations on the system.

The measurements show that the yearly seasonal performance of the system including all electricity consumption and all heat losses of the system, SPF_{SHP} is 2.1, if the yearly space heating demand is 2200 kWh and the yearly domestic hot water consumption is 1640 kWh. The heat distribution pump in the system is usually operated continuously during the heating season and only during domestic hot water production in the summer season. During the test period, the heat distribution pump has been in operation continuously, also in the summer period. When subtraction the electric energy for the heat distribution pump in summer periods when it should not be in operation, the yearly seasonal performance factor increases to 2.4. The seasonal performance factor increases to 2.6 if the heat distribution pump only operates during space heating and domestic hot water production during the whole year.

The theoretical investigation shows that the calculated seasonal performance factor, SPF_{SHP}, applying similar operation conditions as during the experimental investigations in a typical Danish year is 2.1. The calculated seasonal performance increases to 2.7 if the heat distribution pump only operates during space heating and domestic hot water production during the whole year.

There is a very good degree of similarity between the experimental and theoretical results.

Further theoretical investigations show that the seasonal performance factor, SPF_{SHP}, will increase to 3.3 by doubling the solar collector area or by reducing the measured tank heat loss coefficient of 5.62 W/K to the theoretically calculated tank heat loss coefficient of 1.22 W/K.

The theoretical investigations clearly show that well-insulated system components are the most cost-effective way to reach high system efficiencies.

The experimental results also show that the power uptake from the ground is 10 – 20 W/m when the heat pump extracts heat from the ground without assistance from the solar collector loop. The power transfer from the solar collector to the ground is 10 – 180 W/m.

One reason for the high-power transfer from the collector to the ground is the larger temperature difference, which increases the heat transfer. Another reason can be the large thermal expansion coefficient of the polymer ground tubes. The thermal expansion may result in a better contact to the ground in periods with solar to ground operation due to higher fluid inlet temperatures and thermal contraction may result in a worse contact to the ground due to lower fluid inlet temperatures in periods with heat pump alone operation.

Finally, the experimental results for investigated system design indicate that the solar collector area of 6.55 m^2 is too low to maintain the temperature levels in the ground storage.

Nomenclature

Symbols

η_0	Peak collector efficiency	[-]
η	Solar collector efficiency	[-]
a_1	Solar collector heat loss coefficient	[$W/m^2/K$]
a_2	Solar collector heat loss coefficient	[$W/m^2/K^2$]
T_m	Mean collector fluid temperature	[°C]
T_a	Ambient temperature	[°C]
T	Temperature	[°C]
TS1-TS4	Temperatures in ground	[°C]
Φ	Incidence angle	[-]
k_Φ	Incidence angle modifier for beam radiation	[-]
S	Coefficient for incidence angle modifier	
G_t	Total solar irradiance on collector	[W/m^2]
G	Global solar radiation	[kWh/m^2]
Q	Thermal energy	[kWh]
E, P	Electrical energy	[kWh]
SPF	Seasonal performance factor	[-]

Subscripts

HP	Heat pump
ctr	Control system
Sol, Solar	Solar
CPHS	Circulation pump heat source
CPSolar	Circulation pump solar collector loop
CPDist	Circulation pump in heat distribution loop
SHP	Solar heat pump

bst	Before storage
HP+HS	Heat pump plus heat source
e	Heat pump evaporator, heat pump compressor
c	Heat pump condenser
DHW	Domestic hot water
SH	Space heating
AUX	Auxiliary
M	Measured
C	Calculated

References

[1] M. Miara, D. Günther, R. Langner, S. Helmling, 'Efficiency of Heat Pumps in Real Operation Conditions – Results of three Monitoring Campaigns in Germany', ResearchGate, 2014.

[2] J. C. Hadorn, 'Solar and Heat Pump Systems for Residential Buildings', Print ISBN: 978-3-433-03040-0, 2015.

[3] AB Svenskt Klimatneutralt Boende (2019), EP2619509
https://register.epo.org/application?number=EP11827049

[4] Sundberg, J. (1991). *Termiska egenskaper i jord och Berg.* Linköping: Statens geotekniska institut.

https://www.swedgeo.se/globalassets/publikationer/info/pdf/sgi-i12.pdf

[5] Kusuda, T. and P.R. Achenbach. 1965. 'Earth Temperatures and Thermal Diffusivity at Selected Stations in the United States.' *ASHRAE Transactions*. 71(1): 61-74.